Characterization of Substation Process Bus Network Delays

André dos Santos, Bruno Soares, Fan Chen, *Member, IEEE*, Martijn Kuipers, Sérgio Sabino, António Grilo, *Senior Member, IEEE*, Paulo Pereira, *Senior Member, IEEE*, Mário Nunes, *Senior Member, IEEE* and Augusto Casaca, *Life Senior Member, IEEE*

***Abstract*—The paper presents the characterization of network delays in an IEC61850 process bus substation area network, both through theoretical analysis and simulations. Several design targets were defined considering the recommendations of standards and good design practices: number of network hops; total network delay; probability of the delay being exceeded; link load; network topology and availability. An analytical delay estimation methodology is proposed, considering both the steady-state traffic and traffic resulting from a breaker failure event. A complete substation is taken as example for characterizing the network delays, considering a star network topology. Simulations allow obtaining the cumulative distribution functions and percentile values of network delays. Results show a good agreement between the simulation and the analytical analysis. While the delay is best characterized statistically through simulation, finding the maximum network delay through simulations can be very time consuming, making the analytical analysis more suitable.**

***Index Terms*— Communication Delay, Generic Object Oriented System Event, IEC 61850, Power Systems, Precision Time Protocol, Process Bus, Sampled Values.**

I. Introduction

SUBSTATION Automation Systems (SAS) to be used in transmission and distribution networks in the future will be designed to fully support the IEC 61850 communication standard [1]. Accordingly, process bus communication networks will support all critical protection and automation functions, including tripping and blocking commands, which implies that a thoughtful understanding of their behavior and performance for several working conditions is required.

Several studies have been published introducing ways to characterize network delays in SAS networks. Following an experimental approach, Ingram et al. [2] have setup a small scale substation test bed environment, integrating real protection and network equipment, a network impairment emulator and a Real Time Digital Simulator (RTDS) for power system simulation. The delay performance of the network and its impact on the synchronization and protection mechanisms was extensively studied. An important conclusion is that configuration of multicast addresses is important to minimize overhearing of Generic Object Oriented System Event (GOOSE) messages. More recently, Chen and Crossley [3] have evaluated the performance of protection functions in a process bus featuring the Parallel Redundancy Protocol (PRP). The test bed emulates a single bay network comprising Ethernet switches, which interconnects multi-vendor Merging Units (MUs) and Intelligent Electronic Devices (IEDs). The power system was emulated by means of an RTDS.

Huang et al. [4] have proposed a bounded model for communication network delay in wide-area and substation-area protection schemes during steady-state conditions, but did not consider the network behavior during critical events. In this study, all bays were equal, all links supported 1 Gbit/s and all traffic was broadcast to the entire network, although most common IEDs only have 100 Mbit/s Ethernet interfaces. This highlights the need for multicast filtering to prevent overloading the network links, even for small substations, as recommended in [5].

A different traffic delay characterization and impact factor analysis was presented by Gao and Liu [6]. The study used the OPNET Modeler software suite [7] to simulate a simple star topology with 10-BaseT Ethernet links, with a single switch connecting 16 bay level IEDs and two substation monitoring stations. All traffic flows, including Manufacturing Message Specification (MMS), Sampled Values (SV) and GOOSE, were considered to share the same switch. However, no specific traffic models were developed and there was no attempt to simulate the communication network behavior during critical events such as power system faults. All traffic was assumed to be encapsulated in TCP/IP. This work studied the influence of several factors regarding end-to-end delay, including message size, message rate, background traffic and network configuration. A similar study, albeit more limited, but now considering the transmission of real-time traffic directly over Ethernet, was presented by Das et al. [8]. The latter considered 18 IEDs, one substation monitoring host and a server. In a more recent work by the same team [9], the end-to-end delay performance of substation level communications is again evaluated using OPNET. The simulated substation comprises 12 IEDs and the tests span different 10-BaseT Ethernet topologies (cascaded, ring, star, star-ring and redundant ring) and message sizes. No specific traffic models were developed – the simulations were made with a videoconference traffic model.

A different OPNET simulation study was presented by Kumar et al. [10], considering a slightly more complex

A. Santos, B. Soares, F. Chen are with R&D NESTER, Sacavém, Portugal (corresponding author e-mail: andre.santos@ren.pt). M. Kuipers, S. Sabino are with INOV, Portugal. A. Grilo, P. Pereira, M. Nunes and A.Casaca are with INESC-ID, Instituto Superior Técnico, Universidade de Lisboa, Portugal and INOV, Portugal.

This work was supported by CEPRI (Chinese Electric Power Research Institute), in the scope of the R&D Nester (Centro de Investigação em Energia REN-SGCC, SA) project "Substation of the Future".

topology, with two bay star Ethernet Local Area Networks (LAN) interconnected by a router. Two Ethernet data rates were tested: 10 Mbit/s and 100 Mbit/s. A mix of five traffic types was considered, including GOOSE and SV, with different priorities assigned to different message types. It was shown that strict priority scheduling allows higher loads to be supported in small substations, even for 10 Mbit/s links, while 100 Mbit/s was shown to be more stable in general and especially beneficial when the substation comprises multiple bays.

Georg et al. [11] have characterized the SV and GOOSE message delay based on Network Calculus and simulation with the OPNET Modeler. Two scenarios were studied for a single bay LAN, with a switched 100 Mbit/s Ethernet star topology: SV traffic only and SV plus GOOSE traffic. The impact and constraints imposed by the Precision Time Protocol (PTP) are not taken into account.

End-to-end communication delay inside IEC 61850 substations has also been evaluated by Golshani et al. in [12] based on the freeware OMNET++ simulator [13]. A substation comprising three bays with a total of 14 IEDs, a Station PC and a server was simulated. The considered topology is Ethernet star in each bay and another Ethernet star interconnecting the bays, Station PC and server. Both 10 Mbit/s and 100 Mbit/s were considered.

All these works focused on characterizing the network performance, but by lacking a functional description of the protection and automation functions, results may differ significantly from reality. During a power system event, combined process bus background traffic with spontaneous event driven traffic will coexist, affecting network performance, e.g., simultaneous messages publishing by different IEDs may result in traffic congestion. A more realistic simulation study based on OMNET++ is presented by León et al. in [14]. A substation with 9 bays of 4 IEDs each is considered. Detailed IEC 61850 procedures were modeled, specifically regarding GOOSE and SV traffic. Simulation of critical events is considered, comparing the standard substation architecture (star of stars, as already described) with the single switch architecture. The authors also present a scalability study (maximum number of IEDs allowed per bay) and a small scale experiment is also run and compared with simulation results.

More complete network characterization through simulation requires the combination of power system and Information and Communications Technologies (ICT) system modeling for analyzing the mutual impact between domains. The systems may either be modeled in a given simulation environment [15] or split into different environments [16][17][18] by means of joint and synchronized simulation, allowing the benefit of using the most appropriate models from each simulation environment.

An integrated simulation model of power system protection schemes and IEC 61850 process bus communication models was recently published by Santos et al. in [19]. The present paper extends that work, by analyzing a substation with 14 bays and 152 IEDs in terms of network performance, including a detailed characterization of network delays, estimation of the maximum traffic delay and probabilistic delay analysis. As far as the authors know, this is the first time that a substation of this size is considered for network performance analysis under fault event situations.

The rest of the paper is organized as follows. First, the network design objectives are explained. Then, an analytical methodology to determine the maximum network delay for a trip scenario is proposed. SV traffic and GOOSE traffic resulting from the trip is considered deterministic, while other GOOSE traffic and PTP traffic is not, but corresponds to a very small fraction of the total network traffic. The proposed analytical methodology also allows dimensioning the speed of the network links. The analytical methodology is applied to a substation scenario with different types of bays. The analytical results are then compared with the corresponding network simulation, confirming its applicability. A scalability analysis concludes the paper.

II. Design targets

In the substation process bus, the only existing traffic types that can exist are SV, GOOSE and PTP. For the design of the process bus communication network, five network design targets, related with: i) number of hops; ii) total delay; iii) probability of exceeding the delay; iv) link load; and v) availability, are considered.

Concerning the number of network hops, the maximum allowed is 16 hops in order to achieve PTP IEEE 1588 clock precision (Annex B of [20]).

Total delay is an important factor to fault clearance time, which may increase either because of delayed protection action due to high SV communication latency or because of delay tripping due to high GOOSE tripping latency. In this work, a maximum of 3 ms end-to-end delay is used as specified in section 11.2 of IEC 61850-5 [1] for trip messages, where only 20 % (600 µs) of that can be due to the network. The remaining 80 % is reserved for the processing delay in transmitting and receiving IEDs, section 8.2.1 of IEC 61850-10 [21]. This is confirmed in section 11.2.5 of IEC 61850-90-4 [5].

As regards the link load, there are four types of traffic in the network: i) non-periodic GOOSE traffic produced by some event, such as a power system fault; ii) periodic traffic produced by SV sources; iii) background periodic GOOSE traffic not related to that event; and iv) background periodic PTP traffic. In a substation, most of the traffic is of the SV type. An example is shown in Fig. 1, where the first part of the sampling period is filled with SV packets with different offsets and the final part of the sampling period can have other packets. So, the worst case of the network delay is for a GOOSE event to occur at the beginning of an SV cycle, immediately after all SV packets of that cycle have been generated, triggered by the sampling clock. Consequently, this traffic is considered deterministic. Even though most of the traffic is considered deterministic, for the network design, a 74 % load limit cap is chosen as a conservative safety margin.

To account for stochastic traffic in the network design, a

10^{-6} probability of exceeding the maximum delay target is set. Accordingly, it is assumed that a message that has an excessive delay will be considered as a communication failure. This probability is in accordance with typical failure rate values of the most reliable devices in the substation [22].

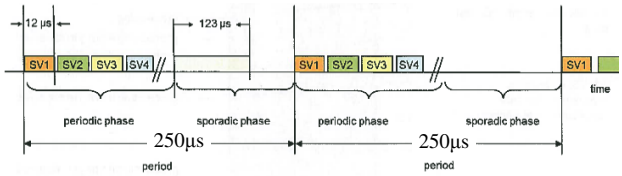

Fig. 1. Example of SV traffic at 4000 Hz (adapted from figure 10 of [5]).

High network availability requires the use of redundancy mechanisms such as the High-availability Seamless Redundancy (HSR) ring or PRP star topologies [23]. The PRP star topology has better real-time performance, as the link load is lower. For this reason, only the PRP star topology is considered in this paper. So, in our study, a switched Ethernet topology is assumed, hence all links are full duplex and no frame collisions may occur.

III. Delay Estimation Analytical Methodology

The total network delay is the time from the instant the first bit starts to be transmitted from the source device until the last bit reaches the destination device. The first device queuing delay is considered to be included in its protocol stack (which represents 40 % of the delay limit).

The total network delay encompasses the processing time T_{pc}, the transmission time T_t, the queuing time T_q and the propagation time T_{pp}.

A. Processing time delay

The processing delay corresponds to the time an Ethernet switch takes to decide to which output port the packet should be sent. A minimum of 7 µs time for a single switch is considered, corresponding to the worst case of several switches analyzed [24]. The simulator's Ethernet switch model considers that packets arriving to the switch are processed at a fixed processing rate of 500,000 packet/s (by default) before being placed in the appropriate link outgoing queue. A fixed 5 µs processing delay per packet was considered in the simulator in addition to the delay caused by the fixed processing rate (2 µs per packet).

B. Transmission time delay

The transmission delay is the time it takes to transmit an Ethernet frame at the line transmission rate in each hop. TABLE I shows typical SV packet sizes at the physical layer (including Ethernet preamble, priority tag, PRP or HSR fields, security extensions, and minimum inter-frame gap), according to [25]. TABLE II shows two examples of GOOSE packet sizes at the physical layer, transfer time class and transfer time, where Type A corresponds to a trip message and Type B to a switchgear position status message.

The transmission time T_t is given by:

$$T_t = \frac{L.8}{R} \quad (1)$$

where L is the packet size (length) in bytes from TABLE I or TABLE II and R is the link rate in bit/s.

TABLE I : Typical SV packet sizes

SV stream	Period [µs]	Packet Size [Byte]	Rate [bit/s]
F4000S1I3U0	250	139	4 448 000
F4000S1I3U3	250	163	5 216 000
F4800S2I3U0	416.7	195	3 744 000
F4800S2I3U3	416.7	245	4 704 000
F12800S8I3U3	625	727	9 305 600
F14400S6I3U3	416.7	567	10 886 400

TABLE II: Examples of GOOSE packet sizes, transfer time class and transfer time

Type	Packet Size [Byte]	Transfer Time Class	Transfer Time [ms]
Type A (trip)	230	TT6	3
Type B (status)	309	TT5	10

Since there may be different message sizes involved during an event, the largest GOOSE message is considered as the worst case. If there are links with different link rates along the path, the slowest rate is considered as the worst case.

C. Queuing time delay

The queuing delay is the time a packet waits in a switch queue before its transmission starts and may vary significantly according to the network load.

For estimating the queuing delay and the probability of exceeding it, design targets ii) and iii), it is necessary to determine how much SV, GOOSE and PTP traffic is going through the links along the path from a source device to a destination device during an event. Additionally, the total number of possible sources and the probability of several sources transmitting simultaneously in an SV period have to be considered, being both protection scheme dependent.

As regards SV traffic, packets are aggregated at each Ethernet switch; therefore they are delayed to a different offset within the SV sampling period (Fig. 1) by the switch queue.

For PTP traffic, only one-step clocks are considered as recommended in section 5.7.1 of IEEE Std C37.238 [20]. Ethernet switches are considered to support peer-to-peer transparent clock on all ports. Considering the peer delay mechanism, there is a "PDelay_Req" and a "PDelay_Resp" message in each direction per hop. Accordingly, 2 PTP sources per hop exist. For the downstream direction, a master clock will generate additional "Sync" and "Announce" messages. Since all paths involved in a trip have at least one hop downstream, the worst case is considered, which corresponds to the number of PTP sources S_{PTP} equal to:

$$S_{PTP} = 2(H + 1) \quad (2)$$

where H is the number of hops. If two-step clocks were considered, additional Follow_Up messages and per slave clock (IED) Delay_Req and Delay_Resp messages would have to be considered resulting in:

$$S_{PTP} = 3(H + 1) + IED \quad (3)$$

where IED is the number of existing IEDs in the substation.

As regards the PTP messages period T_{PTP} and the steady-state GOOSE messages period T_0, the former messages are published every second, while the latter are typically

published every 5 to 30 seconds. Accordingly, between two consecutive GOOSE messages with period T_0, on average, there are T_0/T_{PTP} messages from each PTP source. Consequently, the equivalent number of traffic sources S to be considered for a T_0 period is given by:

$$S = S_G + \frac{T_0}{T_{PTP}} S_{PTP} \quad (4)$$

where S_G denotes the number of GOOSE sources not involved in a trip.

Similarly, the number of SV messages m within a T_0 period is given by:

$$m = \frac{T_0}{T_{SV}} \quad (5)$$

where T_{SV} is the SV message period and may assume any of the values from TABLE I depending on the SV stream.

Considering a given SV period where an event occurs, the probability P of having k or more messages being generated coincidently from a set of S independent sources with random uniform distribution, where all m intervals are equally probable, is given by a binomial distribution:

$$P = \sum_{i=k}^{S} C_i^S \left(\frac{1}{m}\right)^i \left(1 - \frac{1}{m}\right)^{S-i} \quad (6)$$

A uniform distribution for PTP messages may be assumed, as defined in section 9.5.11.2 of IEEE 1588 [26], since the initial PTP message can fall in any of the m intervals and there is some randomness in the interval between consecutive messages. For GOOSE sources not involved in a trip, a similar assumption is made.

Considering the probability of S sources transmitting simultaneously in an SV period being smaller than 10^{-6}, as per design target iii), TABLE III presents the number k of other sources coinciding in the SV period when the event occurs, which should be considered if T_0=5s. For these messages, we consider the largest GOOSE message (type B) as the worst case.

TABLE III
Number k of simultaneous GOOSE messages that should be considered for S sources so that P<10^{-6} (m=20000 SV intervals per T_0=5s)

S other sources	1	28	366	1421	3383
k coincidences	1	2	3	4	5

Additionally, the deterministic GOOSE traffic produced during an event is also quantified, according to the network topology and type of event considered, as presented in section V, to evaluate the queuing delay.

D. Propagation time delay

The propagation delay T_{pp} is the time a signal takes to propagate in the medium. In an optical fiber, the speed is about 2/3 the speed of light in vacuum. Three standardized fiber link distances are typically considered: i) from the switchyard to the inhouse control room, around 500 m resulting in 2.5 µs delay; ii) between devices installed in the switchyard, around 150 m resulting in 0.75 µs delay; and iii) between devices in the control room, around 5 m resulting in 0.025 µs delay. This last value is neglected.

E. Total network delay

The total network delay T_d is estimated as the sum of the processing, the queuing, the transmission and the propagation delays, for all H hops:

$$T_d = \sum_{h=1}^{H} T_{pc_h} + T_{q_h} + T_{t_h} + T_{pp_h} \quad (7)$$

IV. Application Example

The previously presented design methodology is applied to the substation Protection, Automation and Control (PAC) system presented in Fig. 2. The substation comprises two voltage levels, each having a double busbar with bus coupler arrangement, and two power transformers.

High Voltage (HV) bays are labeled from 601 to 609. Bay 601 represents the bus coupler, bays 602 and 603 transformers bays, bays 604 to 609 feeder bays. Extra High Voltage (EHV) bays are labeled 201 to 205, where bay 201 is the bus coupler, bays 202 and 203 are transformer bays and bays 204 and 205 feeder bays. The PAC system encompasses different IEDs that are described in TABLE IV.

TABLE V shows the number of IEDs of each type for each bay and the number of existing bays. Only critical devices are duplicated to achieve high availability performances.

TABLE IV: PAC IEDs

IED	Type	Description
M	critical	Main protection
CBC	critical	Circuit breaker controller and breaker failure
PTC	critical	Power transformer controller
MUPAC	critical	Merging unit for protection
BBP	critical	Busbar protection
COMM	critical	Teleprotection interface
MUMPQ	non critical	Merging unit for metering and control
PQ	non critical	Meter or power quality device
IUDS	non critical	Disconnect switch controller

TABLE V: Existing IEDs per Bay Type in the Substation

Bay Type	#Bays	# IEDs per bay
Bus Coupler	2	2×CBC, 4×MUPAC, 2×MUMPQ, 3×IUDS, 2×M,1×PQ
Feeder	8	2×CBC, 2×MUPAC, 1×MUMPQ, 2×IUDS, 2×M, 1×PQ
Transformer EHV	2	2×CBC, 2×MUPAC, 1×IUDS, 2×M, 2×PTC
Transformer HV	2	2×CBC, 4×MUPAC, 1×MUMPQ, 1×IUDS, 1×PQ

Most process bus traffic messages, i.e. GOOSE and SV, are confined to the same bay, meaning that their source and subscribers belong to the same bay. However, some of this traffic is also subscribed by devices from other bays or located at the station level. Among those traffic messages are the SV bay current measurements (named as SVMUPAC1 and SVMUPAC2) published by the MUPAC of all bays and used by the BBP, or the SV bus voltages published by the MUPAC in the bus coupler bay and used by all feeder bays when closing the circuit breaker controlled by the Synchro-check function. This also happens to some GOOSE messages, e.g., the breaker failure trip command GOOSE type A, published by the CBC devices and subscribed by the BBP to achieve correct busbar trip. Examples of traffic confined to the bay are

SVMUPAC3 and SVMUPAC4, corresponding to the power transformer neutral current measurements.

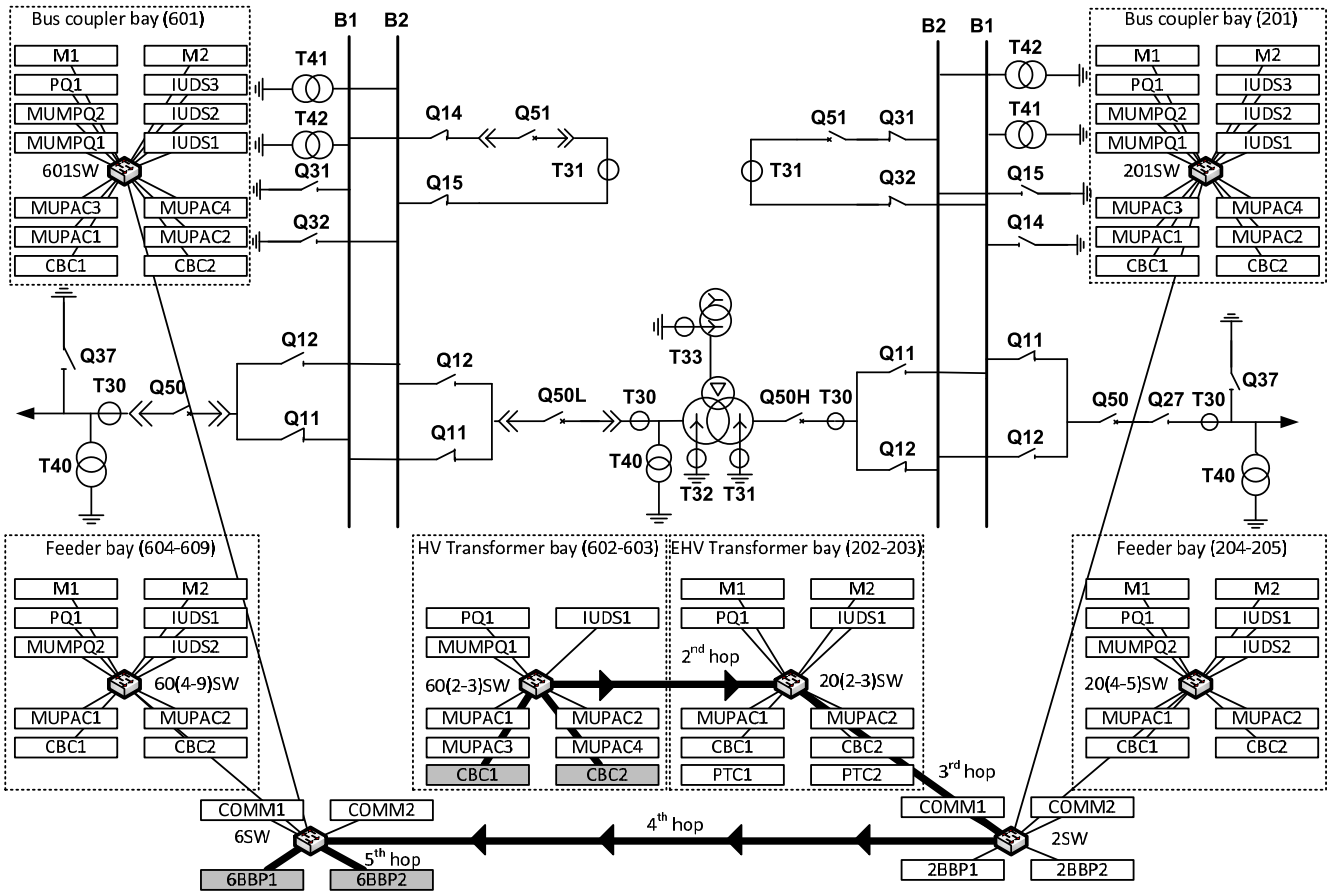

Fig. 2. Substation topology and corresponding process bus protection network. IEDs involved during a Q50L breaker failure trip sent to the HV busbar protections. For readability, only one star of the PRP network is drawn.

As regards the communication network topology, devices are grouped per bay and connected to the corresponding bay switch *n*SW using 100 Mbit/s links, *n* being the bay's number. Substation level devices, such as BBP and COMM are connected to the corresponding substation level *l* central switch *l*SW using 1 Gbit/s and 100 Mbit/s links respectively.

The process bus network has a star topology per voltage level as shown in Fig. 2. A special case is used in the transformer bays because the transformer differential protection subscribes the current measurements from the MU located on both sides of the transformer. In this case, the HV bay Ethernet switch is directly connected to the corresponding EHV bay Ethernet switch, reducing the number of hops and the SV traffic flowing between substation level central switches. Substation level switches are linked among them to guarantee the required traffic path between both voltage levels.

Ethernet multicast traffic filtering is configured statically in each Ethernet switch port, so that only the traffic destined to devices connected to that port goes through. The same Ethernet priority level 4 was assigned to all traffic as recommended in Annex C of IEC 61850-8-1 [27].

Maximum queuing delays and link loads, observed in this system, are characterized analytically and numerically. As regards numerical calculation, the Riverbed Modeler simulator [7], formerly known as OPNET, was used by means of integrated simulation of power system and ICT system [19]. This included a highly abstracted modeling of the power system encompassing a logic description of: i) the substation busbar topology and associated circuit breakers; ii) the number of bays, including its physical location in the substation; and iii) the bay location of power transformers.

Additionally, a detailed implementation was made of the Ethernet protocol and the communication standard IEC 61850-8 and 9 parts. Traffic partitioning was implemented by proper multicast filtering at the Ethernet switches.

V. Delay Estimation Analytical Analysis

It is expected that the maximum delay of a GOOSE message in the system will happen on the occurrence of a power system event, when a burst of GOOSE traffic is generated by the IEDs.

From the different power system events that can occur, the worst case is a transformer trip followed by a HV breaker failure, see Q50L in Fig. 2. During this event, the breaker failure function, in the highlighted CBC1 and CBC2 devices

in the figure, will issue two redundant breaker failure trip GOOSE type A messages that are subscribed by the 6BBP1 and 6BBP2 devices. Considering the network topology shown in Fig. 2, these GOOSE messages will follow the longest network path possible, i.e. 5 hops:

CBCx→602SW→202SW→2SW→6SW→6BBPx

where x is equal to 1 or 2.

Although the most critical message is the 6BBPx trip command sent downstream to all CBC devices in all HV bays, from the network performance point of view the resulting upstream messages updating the circuit breakers new open status, represent the worst case, as most of the SV traffic is upstream, causing a peak in the upstream network flow.

As a result, with 9 HV bays, there are 9×2=18 CBCs involved in a busbar trip. Based on the traffic matrix, not presented for simplicity, there are 28 other GOOSE sources not involved in the trip and generating traffic to this path.

As there are 5 hops, from (2), 12 PTP sources should be considered and, from (4), a total of S=88 sources not involved in a trip should be considered, for T_0 equal to 5 s. Accordingly, and from TABLE III, k=3 sources coinciding with the trip should be considered, these being GOOSE type B as they are the largest existing messages. The coincident sources will be considered for the full path, although each link in the path should also be guaranteed to have enough free capacity to carry them. Accordingly, these two cases (full path and link-by-link computations) will be analyzed, the first to evaluate the overall queuing delay, and the second to evaluate the network load for each hop.

TABLE VI shows the estimation of the queuing delays and network load, with 1 Gbit/s links, for the second to the fifth hop, considering the existing SV traffic, the GOOSE traffic resultant from a trip and k=3 other sources that may coincide with the SV period where the trip message was sent. For packets shorter than 2 µs, due to the switch processing time, a minimum of 2 µs is considered between consecutive packets.

For SV, a T_{SV}=250 µs period was used according to [25]. The maximum link load is the fraction of this period occupied with packet transmissions.

From the data presented in Table VI it can be concluded that if link 602SW→202SW was at 100 Mbit/s, the network load would be 10 times higher (99 %), which is above the design objective for the maximum link load (74 %). The same happens for the links 202SW→2SW (77 %), 2SW→6SW (94 %) and 6SW→6BBPx (318 %). This requires having all links between Ethernet switches at 1 Gbit/s speed.

As regards IED interfaces, all devices have 100 Mbit/s interfaces, except the BPPs that require 1 Gbit/s interface to support the amount of traffic. This confirms that multicast filtering at Ethernet switches is required to prevent overloading the network links with unnecessary traffic.

Comparing the possible queuing delays for the second, third and fourth hops, most messages are common, because they come from the previous link. This means that no additional queuing delays will happen for packets that go through multiple links. Accordingly, the only additional queuing delay that should be considered for the third link is the SV traffic from MUPAC1,2 (EHV), i.e. 2×2 µs. For the fourth link, only 2 flows are new. For the fifth link, only 14 flows are new.

The maximum queuing delay is estimated by summing up all hops' delays in the path, as shown in TABLE VII.

TABLE VI: Queuing delays and load for 1GBIT/S links

2nd hop : 602SW→202SW		
SVMUPAC1,2 (HV)	F4000S1I3U3	2×1.304 µs → 2×2.000 µs
SVMUPAC3,4	F4000S1I3U0	2×1.112 µs → 2×2.000 µs
MUMPQ	F12800S8I3U3	1×5.816 µs
GOOSE type A		2×1.840 µs → 2×2.000 µs
Hop queuing delay		17.328 µs
Coincident GOOSE messages (type B)		3×2.472 µs
Maximum hop queuing delay		24.744 µs
Maximum link load		9.90 %
3rd hop : 202SW→2SW		
SVMUPAC1,2 (HV)	F4000S1I3U3	2×1.304 µs → 2×2.000 µs
SVMUPAC1,2 (EHV)	F4000S1I3U3	2×1.304 µs → 2×2.000 µs
GOOSE type A		2×1.840 µs → 2×2.000 µs
Coincident GOOSE messages (type B)		3×2.472 µs
Maximum hop queuing delay		19.416 µs
Maximum link load		7.77 %
4th hop : 2SW→6SW		
SVMUPAC1,2 (HV)	F4000S1I3U3	4×1.304 µs → 4×2.000 µs
GOOSE type A		2×2×1.840 µs → 2×2×2.000 µs
Hop queuing delay		16.000 µs
Coincident GOOSE messages (type B)		3×2.472 µs
Maximum hop queuing delay		23.416 µs
Maximum link load		9.37 %
5th hop : 6SW→6BBPx		
SVMUPAC 1,2	F4000S1I3U3	18×1.304 µs → 18×2.000 µs
GOOSE type A		18×1.840 µs → 18×2.000 µs
Hop queuing delay		72.000 µs
Coincident GOOSE messages (type B)		3×2.472 µs
Maximum hop queuing delay		79.416 µs
Maximum link load		31.8 %

TABLE VII: MAXIMUM QUEUING DELAY FROM CBCX TO 6BBPX

Links	Delays
602SW→202SW	17.816 µs
202SW→2SW	4.000 µs
2SW→6SW	8.000 µs
6SW→6BBPx	56.000 µs
Coincident GOOSE messages (type B)	3×2.472 µs
Maximum queuing delay	93.232 µs

Finally, an estimation of the maximum total network delay for the breaker failure trip GOOSE can be made using (7). For the processing delay, 4 switches at 7µs are considered. For the queuing delay, the data of TABLE VII is considered. For the transmission delay T_t, the largest message for each link is considered: a F12800S8I3U3 SV message for the second link and a GOOSE type B message for the other links. T_t is determined from (1), considering the first hop at 100 Mbit/s and the others at 1 Gbit/s. For the propagation delay, 1 hop is from the switchyard to the control room, 2 hops are in the switchyard and the other 2 hops are in the control room. Finally the total delay is given by:

$$T_d = 4 \times 7\mu s + 93.232\mu s + \\ +(24.72\mu s + 5.816\mu s + 3 \times 2.472\mu s) + \\ +(2.5\mu s + 2 \times 0.75\mu s) = 163.2\mu s \quad (8)$$

where the 4 terms in the sum correspond to the 4 terms of (7), respectively. The analysis concludes that with probability ($1\text{-}10^{-6}$) the maximum delay is lower than 163.2 µs, which is 27 % of the 600 µs limit.

If two-step clocks were considered, from (3), 170 PTP sources should be considered and from (4), a total of S=878 sources should be considered. From TABLE III, k=4 sources coinciding with the trip should be considered, increasing T_d by 2.472 µs to 165.7 µs, which is 28 % of the 600 µs limit. Thus, it can be concluded that the effect of PTP traffic is negligible, even for two-step clocks.

VI. Numerical Simulation

Numerical simulations in Riverbed Modeler v18.5 [7] were used to statistically characterize the SV and GOOSE traffic delays by means of cumulative distribution function and percentile values.

The simulation timespan was 13.5 s, starting statistics collection after a warmup time of 3.5 s. A single breaker failure event was triggered at 7 s. There were no frame drops observed in the simulations, which would be expected if the link load is below the design target and packet bursts can be accommodated within the existing Ethernet switch buffers. Each simulation run took 6 minutes wall-clock time on a 2.83 GHz quad-core system with 8 GB of RAM running a 64-bit Linux operating system.

To guarantee accuracy of the results, a convergence analysis of the 98th, 95th and 50th percentile was made with 40 simulation runs. A convergence criterion of having the 95 % confidence interval smaller than 2 % of the average of the obtained results was used. Fig. 3 and 4 show the accumulated results of up to 40 simulations. Just 3 simulations are enough for the convergence of the GOOSE delays, while the SV delays require 8 simulations to converge.

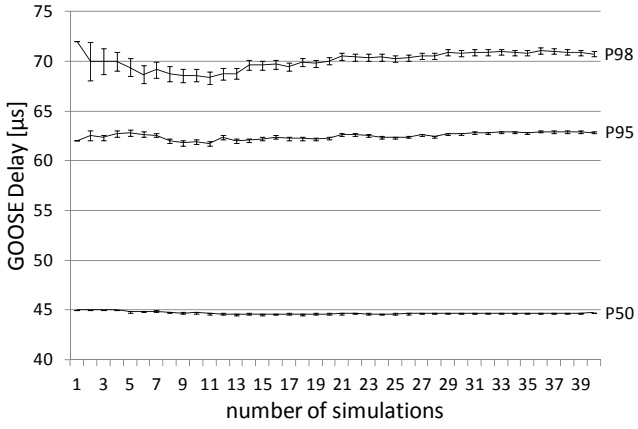

Fig. 3. Convergence analysis of the 98th (P98), 95th (P95) and 50th (P50) percentiles of the GOOSE delay. The 95 % confidence interval is represented by vertical lines.

The cumulative distribution function (CDF) of the SV and GOOSE traffic delays are presented in Fig. 5. The maximum SV and GOOSE message delay recorded in the simulations were 150 µs and 145 µs, respectively, as expected from the previous analytical analysis, although there are a few differences between the analytical analysis and the simulation.

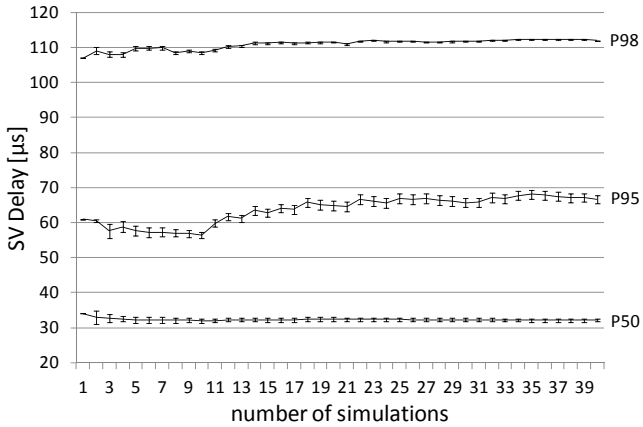

Fig. 4. Convergence analysis of the 98th (P98), 95th (P95) and 50th (P50) percentiles of the SV delay. The 95 % confidence interval is represented by vertical lines.

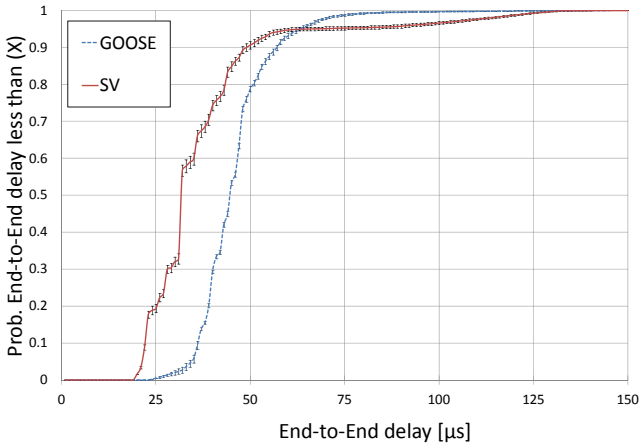

Fig. 5. CDF of End-to-End delay for SV and GOOSE traffic. The 95 % confidence interval is represented by vertical lines.

An aspect that was not taken into account in the analytical analysis is the possibility of having queuing in the source node, as only the network delay was taken into account. Although the probability of having a non-zero queuing delay in the source node is very low, as the first link is, for most IEDs, at 100 Mbit/s, if there is queuing delay it can be as high as tens of microseconds. Finally, the simulation analysis did not consider the simulation of PTP traffic, as the analytical analysis did. However, the effect of PTP traffic is minimal, as PTP sources generate just 1 packet/s of each type, resulting in a very low traffic load as compared with the SV traffic load.

Results presented in Fig. 5 indicate that for 95 % of the overall traffic, SV has lower delays than GOOSE messages. This is due to the higher weight of intra-bay SV traffic.

TABLE VIII shows detailed statistics for GOOSE and SV traffic: 50th, 95th, 98th percentiles. Results include their average, standard deviation and the 95 % confidence interval. From Fig. 5, it can be seen that the SV CDF is nearly horizontal near the 95th percentile, explaining the large variations of the 95th percentile delay.

TABLE VIII
END-TO-END DELAY STATISTICS FOR GOOSE AND SV TRAFFIC CONSIDERING 40 SIMULATION RUNS

Percentile	Statistic	GOOSE [µs]	SV[µs]
98 %	Average	70.8	111.9
	Std. Dev.	0.9	1.4
	Confidence interval	±0.3 (0.4%)	±0.4 (0.4%)
95 %	Average	62.8	66.7
	Std. Dev.	0.3	3.8
	Confidence interval	±0.1 (0.2%)	±1.2 (1.8%)
50 %	Average	44.7	32.1
	Std. Dev.	0.1	0.3
	Confidence interval	±0.0 (0.1%)	±0.1 (0.3%)

Results show that the standard deviation increases with the percentile value, as the higher the percentile, the fewer traffic messages will have longer delays. Nevertheless, the convergence criteria were fulfilled in all percentiles of interest.

VII. SCALABILITY ANALYSIS

TABLE IX shows simulation results for different substation sizes for a brief scalability analysis. The substation previously considered is the Small Substation, with two voltage levels, EHV and HV, of double busbar arrangement (DB) each. The EHV level of the Medium Substation is a double busbar with transfer bus arrangement (DB-TB). The Large Substation has and additional EHV voltage level of breaker-and-a-half arrangement (B&H).

The results show that even for a large substation it is possible to meet the maximum delay requirements. The simulation analysis is not capable of finding this worst case maximum, particularly for the large substation, where 10 simulation runs took a day to complete and found a smaller maximum delay than 40 runs of the medium substation.

TABLE IX
SUBSTATIONS SIZES CONSIDERED FOR SCALABILITY ANALYSIS AND CORRESPONDING COMPUTED DELAYS

Parameter	Small Substation	Medium Substation	Large Substation
Number of EHV bays	2 (DB)	5 (DB-TB)	10 (B&H) 5 (DB-TB)
Number of HV bays	5 (DB)	10 (DB)	17 (DB)
Total number of IED	152	274	570
Analytical max. delay	163 µs	219 µs	312 µs
Simulation runs	40	40	10
GOOSE maximum delay	145 µs	163 µs	158 µs
GOOSE delay P98	70.8±0.3 µs	96.1±0.5 µs	105.7±0.8 µs
GOOSE delay P95	62.8±0.1 µs	80.0±0.1 µs	88.4±0.5 µs
GOOSE delay P50	44.7±0.0 µs	57.0±0.0 µs	61.2±0.2 µs
SV maximum delay	150 µs	165 µs	150 µs
SV delay P98	111.9±0.4 µs	121.2±0.3 µs	124.2±0.3 µs
SV delay P95	66.7±1.2 µs	90.5±0.8 µs	88.9±0.8 µs
SV delay P50	32.1±0.1 µs	37.4±0.1 µs	38.0±0.4 µs

VIII. CONCLUSIONS

This paper presented a methodology for designing IEC 61850 process bus networks used by critical PAC systems in large substations and considering the sequence of events in faults situations. Several guidelines for building the substation process bus network are presented considering five network design targets: the number of hops, total delay, probability of exceeding the delay, link load and availability.

As the existing SV and GOOSE traffic has periodic and stochastic characteristics, two methodologies for traffic delay estimation were presented. The first is an analytical methodology capable of characterizing the maximum expected delay observed in the system, and the second is a simulation methodology capable of characterizing the traffic delay by means of: average value, cumulative distribution function and percentile values. As explained, both methodologies are required to fully characterize SV and GOOSE traffic, since neither the analytical methodology is capable of determining the resulting cumulative distribution function, nor the simulation methodology is capable of determining the maximum expected delay value.

An application example of delay traffic characterization in a complete substation network topology was made, in which both analytical and simulation results show that the design targets can be met. A good agreement between analytical and simulation results was achieved. In the example shown, it was concluded that links between Ethernet switches should be at 1 Gbit/s speed, while most IEDs only have 100 Mbit/s interfaces, requiring multicast traffic filtering at Ethernet switch ports. The analytical analysis concludes that with probability ($1\text{-}10^{-6}$) the maximum network delay is lower than 163 µs, which is 27 % of the 600 µs limit imposed by IEC 61850. The weight of non-deterministic traffic is less than 5 % of the total delay. The numerical simulation found a maximum delay of 150 µs, with the 98^{th} percentile of delay being 70.8 µs for GOOSE traffic and 111.9 µs for SV traffic.

The results of a scalability analysis have been presented for two larger substations. Results show that traffic delay increases with substation size but still respecting the design requirements. Furthermore, multicast filtering at Ethernet switches prevents overloading the network links with unnecessary traffic and consequently a single VLAN for GOOSE, SV and PTP traffic using the same priority level for all these traffic types can fulfill all design targets and requirements from standards.

While the delay is best characterized statistically through simulation, the link load is strongly dominated by SV traffic, being almost deterministic, thus allowing a precise analytical estimation based on the traffic matrix. For finding the maximum network delay, simulations can be very time consuming, making the analytical analysis a better way to find the worst case maximum delay.

This also leads to the conclusion that running simulations is a good way of getting a characterization of network delays using cumulative distribution functions, but finding the worst case maximum delay can be very time consuming, as a single simulation involving a single trip took 6 minutes to complete..

Future work will cover a deeper study of other substations topologies, e.g., breaker-and-a-half; the use of different traffic priority, VLAN and multicast filtering configurations; and co-simulation involving network simulators and power system simulators.

IX. REFERENCES

[1] IEC 61850-5, "Communication networks and systems for power utility automation - Part 5: Communication requirements for functions and device models", Edition 2.0, 2013.

[2] D. Ingram, P. Schaub, D. Campbell, R. Taylor, "Assessment of real-time networks and timing for process bus applications", *Proc. Cigré South East Asia Protection and Automation Conference (SEAPAC'2013)*, Brisbane, Queensland, Australia, March 2013.

[3] Xi Chen, P. Crossley, "Interoperability Performance Assessment of Multivendor IEC61850 Process Bus", *IEEE Transactions on Power Delivery*, vol. 31, no. 4, pp. 1934-1944, August 2016.

[4] C. Huang, F. Li, T. Ding, Y. Jiang, J. Guo, Y. Liu, "A Bounded Model of the Communication Delay for System Integrity Protection Schemes", *IEEE Trans. Power Delivery*, vol. 31, no.4, pp.1921-1933, 8/2016. DOI: 10.1109/TPWRD.2016.2528281.

[5] IEC/TR 61850-90-4, "Communication networks and systems for power utility automation – Part 90-4: Network Engineering Guidelines", Edition 1.0, 8/2013.

[6] H. Gao, W. Jin, G. Liu, "Simulation study on delay of end-to-end data communication for protective relaying in substations", *Frontiers on Electrical and Electronical Engineering in China*, Springer, vol. 3, no. 2, 2008, pp. 246-250.

[7] Riverbed Modeler. http://www.riverbed.com/gb/products/steelcentral/steelcentral-riverbed-modeler.html (Retrieved October 2016).

[8] N. Das, W. Ma, S. Islam, "Analysis of End-to-End Delay Characteristics for Various Packets in IEC 61850 Substation Communications System", *Proc. Australasian Universities Power Engineering Conference 2015 (AUPEC'2015)*, Wollongong, Australia, September 2015.

[9] N. Das, T. Wong, S. Islam, "Analysis of end-to-end delay characteristics among various packet sizes in modern substation communication systems based on IEC 61850", *Proc. Asia-Pacific World Congress on Engineering 2015 (APWCE'2015)*, Plantation Island, Fiji, May 2015.

[10] S. Kumar, N. Das, S. Islam, "Performance Analysis of Substation Automation Systems Architecture Based on IEC 61850", *Proc. Australasian Universities Power Engineering Conference 2014 (AUPEC'2014)*, Curtin, Australia, September-October 2014.

[11] H. Georg, N. Dorsch, M. Putzke and C. Wietfeld, "Performance Evaluation of Time-critical Communication Networks for Smart Grids based on IEC 61850", *IEEE INFOCOM Workshop on Communications and Control for Smart Energy Systems (CCSES)*, Turin, Italy, April 2013.

[12] M. Golshani, G. Taylor, I. Pisica, "Simulation of power system substation communications architecture based on IEC 61850 standard", *Proc. 49th International Universities Power Engineering Conference (UPEC'2014),* Cluj-Napoca, Romania, September 2014.

[13] OMNET++. http://www.omnetpp.org/ (Retrieved March 2017).

[14] H. León , C. Montez, M. Stemmer, F. Vasques, "Simulation Models for IEC 61850 Communication in Electrical Substations Using GOOSE and SMV Time-critical Messages", *Proc. IEEE World Conference on Factory Communication Systems (WFCS'2016)*, Aveiro, Portugal, June 2016.

[15] K. Hopkinson, X. Wang, R. Giovanini, J. Thorp, K. Birman, and D. Coury, "EPOCHS: A Platform for Agent-Based Electric Power and Communication Simulation Built from Commercial Off-The-Shelf Components", *IEEE Trans. on Power Sys.*, vol. 21, no. 2, pp. 548 - 558, May 2006.

[16] R. Bottura, A. Borghetti, F. Napolitano, C. Nucci, "lCT -power Co-simulation Platform for the Analysis of Communication-based Volt/Var Optimization in Distribution Feeders", *Proc. IEEE PES Innovative Smart Grid Technologies Conference (ISGT'2014)*, Washington D.C., USA, February 2014.

[17] A. Borghetti, R. Bottura, M. Barbiroli, C. Nucci, "Synchrophasors-Based Distributed Secondary Voltage/VAR Control via Cellular Network", *IEEE Transactions on Smart Grid*, vol. 8, no. 1, January 2017.

[18] M. Levesque, M. Maier,C. Bechet, E. Suignard, A. Picault and G. Joós, "From Co- Toward Multi-Simulation of Smart Grids based on HLA and FMI Standards: A Telecontrol Case Study Based on Real World Configurations", arXiv:1412.5571v1 [cs.NI] 17 Dec 2014.

[19] A. Santos, B. Soares, F. Chen, M. Kuipers, S. Sabino, A. Grilo, P. Pereira, M. Nunes, A. Casaca, "Integrated Simulation Model of Power System Protection Schemes and Process Bus Communication Networks", *IEEE Electrical Power and Energy Conference (EPEC 2016)*, Ottawa, Canada, 12-14 October 2016.

[20] IEEE Std C37.238™-2011, "IEEE Standard Profile for Use of IEEE 1588™ Precision Time Protocol in Power System Applications", 14 July 2011.

[21] IEC 61850-10, "Communication networks and systems for power utility automation - Part 10: Conformance testing", Edition 2.0, 2012.

[22] A. dos Santos, M.T. Correia de Barros and P.F. Correia, "Reliability and Availability Analysis Methodology for Power System Protection Schemes", in *18th Power Systems Computation Conference*, Wroclaw, August 2014.

[23] IEC 62439-3, "Industrial communication networks - High availability automation networks - Part 3: Parallel Redundancy Protocol (PRP) and High-availability Seamless Redundancy (HSR)", Edition 3.0, 2016.

[24] "Ruggedcom RSG2288 Datasheet", Siemens, 14/2/2016, https://support.industry.siemens.com.

[25] IEC 61869-9, "Instrument transformers Part 9: Digital interface for instrument transformers", Edition 1.0, 2016.

[26] IEEE Std 1588™-2008 (Revision of IEEE Std 1588-2002), "IEEE Standard for a Precision Clock Synchronization Protocol for Networked Measurement and Control Systems", 24 July 2008.

[27] IEC 61850-8-1, "Communication networks and systems for power utility automation – Part 8-1: Specific communication service mapping (SCSM) – Mapping to MMS (ISO 9506-1 and ISO 9506-2) and to ISO/IEC 8802-3", Edition 2.0, 6/2011.

X. BIOGRAPHIES

André dos Santos holds a Doctor degree from the Instituto Superior Técnico, University of Lisbon (IST/UL). He is head of Protection and Automation Conception and Design division in the Portuguese Transmission System Operator. Secretary of CIGRE WG B5.16 and member of CIGRE WG B5.23.

Bruno Soares holds a M.Sc. in Electrical and Computers Engineering in Power Systems from the Faculty of Engineering of Porto University (FE/UP). Since September 2015, Bruno is with R&D Nester, as a Research Engineer in the areas of substation's secondary systems and communication networks.

Fan Chen (M'12) received the M.E. degree in power system automation from SouthWest Jiao Tong University of China in 2007. He is a senior engineer in China Electric Power Research Institute (CEPRI) which belongs to State Grid Corporation of China. His research areas are smart substation and IEC61850.

Martijn Kuipers got the Ph.D. in Electrical Engineering from Aalborg University, Denmark. He is currently a senior researcher at INOV-INESC, Portugal.

Sérgio Sabino received his M.Sc degree in Informatics Engineering from University of Algarve, Portugal. Currently he is a PhD student of Electrical and Computer Engineering programme at University of Lisbon-Instituto Superior Técnico and also a junior researcher at INESC-ID, Lisbon.

António M. R. C. Grilo got the Ph.D. in Information and Computer Engineering at Instituto Superior Técnico, Portugal, where he is currently Assistant Professor. He is a member of the Research Group in "Communication Networks and Mobility" at Inesc-ID, Portugal, and "Network Architecture" at INOV, Portugal. He is a Senior Member of IEEE.

Paulo Rogério B. A. Pereira (S'97, M'04, SM'15) received his Ph.D. in Electrical and Computer Science Engineering from Instituto Superior Técnico, University of Lisbon (IST/UL), Portugal, in 2003. He is an assistant professor of computer networks at IST/UL and a senior researcher at INESC-ID.

Mário Serafim Nunes got the PhD in Electronics Engineer and Computers from the Instituto Superior Técnico, University of Lisbon, Portugal. Full Professor at Instituto Superior Técnico, Lisbon. From 2001 to 2015 he was Director of INOV, where he is now scientific coordinator of the Telecom Area. He is a Senior Member of IEEE.

Augusto Casaca got the Ph.D. in Computer Science at the University of Manchester, UK. Full Professor at Instituto Superior Técnico, Portugal, presently he is Leader of the Research Group in "Communication Networks and Mobility" at Inesc-ID, Portugal, and "Network Architecture" at INOV, Portugal. He is a Life Senior Member of IEEE.